Supporting Information

Sacchi et al. 10.1073/pnas.1404605111

SI Methods

Recombinant $\alpha_2PI_{1–8}$-$VEGF_{164}$ Production and Purification. The cDNA for mouse $VEGF\text{-}A_{164}$ was PCR-amplified using primers designed to allow for fusion of the transglutaminase substrate sequence NQEQVSPL, comprising the 8 N-terminal residues of α_2-plasmin inhibitor ($\alpha_2\text{-}PI_{1–8}$) onto the N terminus of the amplified cDNA before insertion into the expression vector pRSET (Invitrogen). The fusion protein was expressed in *Escherichia coli* strain BL21 (Dε3) pLys (Novagen). The recombinant $\alpha_2\text{-}PI_{1–8}\text{-}VEGF\text{-}A_{164}$ was isolated from inclusion bodies, processed, and refolded using a slightly modified version of a previously published protocol (1). Briefly, the inclusion bodies were collected from the bacterial lysate by centrifuging, washed with Triton X-114 to remove membrane proteins and endotoxins, and extracted with urea buffer overnight at 4 °C under magnetic stirring. Further dimerization of $\alpha_2\text{-}PI_{1–8}\text{-}VEGF\text{-}A_{164}$ was done with a redox system (0.5 mM oxidized glutathione, 5 mM reduced glutathione) added into the protein solution after the 2 M urea dialysis, and $\alpha_2\text{-}PI_{1–8}\text{-}VEGF\text{-}A_{164}$ was dimerized under stirring for 48 h at 4 °C. Then, glutathione and urea were removed by three sequential dialyses of 24 h against Tris buffers. Proteins were then concentrated using a 10-kDa Amicon tube (Millipore, Merck) and further filtered through a 0.22-μm filter. $\alpha_2PI_{1–8}\text{-}VEGF_{164}$ monomers and dimers were separated using size exclusion with a HiLoad 16/60 Superdex 75-pg column (GE healthcare). Fractions corresponding to $\alpha_2PI_{1–8}$-VEGF dimers were pooled together, concentrated with Amicon tubes, and filtered through a 0.22-μm filter. $\alpha_2PI_{1–8}$-VEGF dimers were verified to be >99% pure by SDS/PAGE and MALDI-TOF analysis. Endotoxin level was verified to be under 0.05 EU/mg of protein using the LAL assay (GenScript).

Fibrin-Gel Preparation. Fibrin matrices were prepared by mixing human fibrinogen (plasminogen-, von Willebrand Factor-, and fibronectin-depleted; Enzymes Research Laboratories), factor XIIIa (CSL Behring), and thrombin (Sigma-Aldrich) combined at different concentrations as described in *Results* with 2.5 mM Ca^{2+} in 4-(2-hydroxyethyl)-1-piperazineethanesulfonic acid (Hepes) (Lonza). Matrices containing aprotinin-$\alpha_2\text{-}PI_{1–8}$ [produced as described (2)] and $\alpha_2\text{-}PI_{1–8}\text{-}VEGF_{164}$ were obtained by adding the engineered proteins to the cross-linking enzymes solution before mixing with fibrinogen. Matrices were allowed to polymerize at 37 °C for 1 h before use or directly injected after mixing to allow in situ polymerization, depending on the experimental design.

$\alpha_2\text{-}PI_{1–8}\text{-}VEGF\text{-}A_{164}$ Release Profile from Fibrin Hydrogels. Fibrin matrices of 50 μL volume were generated with 10 mg/mL fibrinogen, 2 U/mL thrombin, 5 U/mL factor XIII, 5 mM calcium chloride as previously described for this assay (3), and 10 μg/mL $VEGF\text{-}A_{164}$ (R&D Systems) or of $\alpha_2\text{-}PI_{1–8}\text{-}VEGF_{164}$. Fibrin gels were polymerized at 37 °C for 1 h and transferred into 24-wells containing 500 μl of washing buffer. The 100% release control well contained only the growth factor in buffer. Every 24 h, buffers were collected, stored at −20 °C and replaced with fresh buffer. For the 100% release control well, 20 μl of buffer was taken out every day and stored at −20 °C. After 7 d, the cumulative release of growth factor was quantified by ELISA using the 100% released control as reference (DuoSet; R&D Systems).

VEGF-R2 Phosphorylation Assay. Human umbilical vein endothelial cells (HUVECs) (PromoCell) were seeded in 96-well plates (3,000 cells per well) and starved 4 h with serum-free MCDB-131 medium (Invitrogen). Cells were then stimulated with 50 ng/mL $VEGF\text{-}A_{164}$ or $\alpha_2\text{-}PI_{1–8}\text{-}VEGF\text{-}A_{164}$ for 5 min. Phosphorylated VEGF-R2 was quantified with a phospho-ELISA kit. Briefly, ELISA plates were coated with a capture antibody for VEGF-R2 and then incubated with cell lysates. The phosphorylation state was detected with an anti-phospho-tyrosine antibody and normalized to a standard according to manufacturer instructions (phospho-VEGF-R2/KDR, DuoSet IC; R&D Systems).

In Vitro Gel Polymerization. Fibrin matrices of 50 μL volume were prepared onto a plastic minitray (Nunc Microwell Minitrays; Sigma-Aldrich) and placed on ice to slow down gel polymerization. The fibrinogen solution was first deposited into the well with a pipette tip, avoiding the formation of bubbles, and the cross-linking enzyme solution was added. Solutions were mixed three times with the pipette to guarantee homogenous mixing. The start of polymerization was defined by the change of consistency from liquid to stiff as detected by touch with the pipette tip.

Rheology. Fibrin-gel discs of 1-mm thickness were preformed into press-to-seal silicone isolator slides (Invitrogen) coated with parafilm at room temperature. Gels were allowed to polymerize for 1 h at 37 °C, removed from the support, and placed in PBS overnight at 4 °C to allow swelling. Gel stiffness was determined by performing small-strain oscillatory shear rheometry using a Bohlin CVO 120 high-resolution rheometer with plate–plate geometry at room temperature (Instrumat SA). Gels were sandwiched between the two plates of the rheometer with compression up to 80% of their original thickness to avoid slipping. Measurements were then conducted in a constant strain (0.05) mode as a function of frequency (from 0.1 Hz to 10 Hz) to obtain dynamical spectra ($n = 3$ per condition).

Intramuscular Fibrin-Gel Implantation. To avoid an immunological response to human fibrinogen and cross-linking enzymes, 6- to 8-wk-old immunodeficient CB.17 SCID mice (Charles River Laboratories) were used. Animals were treated in accordance with the Swiss Federal guidelines for animal welfare, after approval from the Veterinary Office of the Canton of Basel-Stadt (Basel, Switzerland). A liquid volume of 50 μL was aspirated rapidly with a 0.3-mL insulin syringe with integrated 30 G needle (Becton Dickinson) and injected into the gastrocnemius muscle of the mice previously anesthetized with 3% isofluorane inhalation. After injection, in situ polymerization was allowed for 20 s before slowly extracting the needle.

In Vivo Multispectral Imaging. Fibrin gels were prepared as previously described, but fluorescent Alexa 647-conjugated fibrinogen (Invitrogen) was included at a concentration of 0.5 ng/mL to monitor the degradation of the different fibrin-gel compositions in vivo by noninvasive multispectral imaging. The experiments were performed at the Ludwig Boltzmann Institute after approval by the local ethical committee. Animals were treated according to the National Institutes of Health guidelines. Carprofen (2.5 mg/kg; Pfizer) was administered to animals preoperatively and for the following 3 d to ensure analgesia. A liquid volume of 50 μL was injected into gastrocnemius muscles on both hindlimbs of BALB/c nu/nu nude mice ($n = 10$ per group). The fluorescence of the fibrin matrix was noninvasively followed and quantified over a period of 9 d using a multispectral imaging system (Maestro Imaging System; CRI). Regions of interest were defined and analyzed. The signal (given as counts per s) was normalized to the values obtained on day 1 and expressed as a percentage.

Histological Analyses. Mice were anesthetized with Ketamin (100 mg/kg) and Xylazin (10 mg/kg) i.p. and euthanized by vascular perfusion of 1% paraformaldehyde (PFA) (Sigma-Aldrich) in PBS (pH 7.4) for 3 min under 120 mm/Hg of pressure. Gastrocnemius muscles were harvested, postfixed in 0.5% PFA in PBS (pH 7.4) for 2 h at room temperature, and cryoprotected in 30% (wt/vol) sucrose in PBS at 4 °C overnight. Muscles were embedded in optimal cutting temperature (OCT) compound (CellPath), frozen in freezing isopentane, and cryosectioned. Tissue sections were stained with H&E to verify the intramuscular localization of the gel. Vascular morphology was analyzed by immunofluorescence staining on 12-μm-thick frozen sections cut along the longitudinal axis. The following primary antibodies and dilutions were used: rat anti-mouse CD31 (clone MEC 13.3; BD Biosciences) at 1:100; mouse anti-human α-SMA (clone 1A4; Sigma-Aldrich) at 1:400; and rabbit anti-rat NG2 (Millipore, Merck) at 1:200. Fluorescently labeled secondary antibodies (Invitrogen) were used at 1:200. Fluorescence images were taken with a 40× objective on a Carl Zeiss LSM710 3-laser scanning confocal microscope (Carl Zeiss).

In some experiments, the amount of nondegraded gel was assessed histologically by immunostaining with a primary antibody that specifically recognizes fibrin, but not fibrinogen (mouse anti-human fibrin, clone E8; Beckman Coulter Immunotech) at a dilution of 1:200. Tissue sections were obtained at 250-μm intervals, in three muscles per group ($n = 3$). Images were taken in each section where gel was detectable with a 10× objective on an Olympus BX61 fluorescence microscope (Olympus) and merged using the multiple image alignment (MIA) function of the CellP imaging analysis software (Olympus) to reconstruct the total area of the tissue section in which the nondegraded gel was present. The total surface area occupied by nondegraded gel was quantified (in mm^2) using ImageJ software (http://rsb.info.nih.gov/ij/) as the sum of all sections in each analyzed muscle.

In some experiments, physiological perfusion of induced vessels was assessed by intravascular staining with a fluorescently labeled *Lycopersicon esculentum* (tomato) lectin (Vector Laboratories) that binds the luminal surface of blood vessels, as previously described (4). Briefly, mice were anesthetized, and lectin was injected i.v. (50 μL of a 2 mg/mL lectin solution per mouse) and allowed to circulate for 4 min before vascular perfusion of 1% PFA in PBS (pH 7.4) for 3 min under 120 mm/Hg of pressure.

Vessel Measurements. Vessel diameters and vessel length density (VLD) were measured in muscle cryosections after immunostaining for CD31, NG2, and SMA as previously described (4, 5). Briefly, vessel diameters were measured by overlaying captured microscopic images with a square grid. Squares were selected randomly, and the diameter of each vessel, if present, in the defined square was measured (in μm). Around 500 total diameter measurements were obtained from three independent muscles for each group ($n = 3$). VLD was measured in 5–10 fields per muscle from three muscles per group ($n = 3$) by tracing the total length of vessels in each field and dividing it by the area of the field (mm of vessel length/mm^2 of surface area). All analyses were performed using the Cell P imaging software (Olympus).

Subcutaneous Fibrin-Gel Implantation. All animal procedures were approved by the Cantonal Veterinary Office of Canton Zurich (Zurich, Switzerland). Female Crl:CD1 Foxn1^{nu} nude mice were used at 4–5 wk of age. Gel implantation and excision was performed as described (6). Briefly, animals were anesthetized by inhalation of 2% isofluorane. The dorsal skin was disinfected with 70% ethanol. Two incisions, ∼1.5 cm long, were made along the left and right sides of the dorsum. Four gels of 20 μL volume were implanted in each mouse in a random order, a 10–0 Dafilon suture (Braun) was placed through each fibrin-gel pellet to fasten the gel to the s.c. area just beneath the skin, and wounds were closed with 7–0 Prolene sutures (Ethicon). Animals were euthanized 14 d later by carbon dioxide asphyxiation. Gels were excised together with the surrounding skin, and samples were stored at −80 °C for further analysis.

α_2-PI$_{1-8}$-VEGF-A$_{164}$ Protein Extraction and Quantification. The concentration of α_2-PI$_{1-8}$-VEGF$_{164}$ in the gels after in vivo implantation was measured from explanted and frozen fibrin gels as described (6). They were washed in PBS for 8 h at 4 °C, changing the PBS every hour. Afterward, 50 mU of plasmin (Sigma-Aldrich) in 50 μL of deionized water were added to each gel and incubated at 37 °C on a shaker at 1,000 rpm. After 8 h, the plasmin solution was renewed and incubation at 37 °C on a shaker continued until all gels were completely dissolved (∼48 h). The amount of VEGF in the resulting samples was measured using an ELISA kit (R&D Systems). One hundred microliters of each sample was used in triplicate, and the assay was performed according to the manufacturer's instructions.

Endothelial Cell Proliferation Assay. VEGF biological activity was assessed in a HUVEC proliferation assay as described (6). Cells were cultured in 96-well plates (5,000 cells per well) in EGM-2 fully supplemented growth medium (Lonza) in 5% CO_2 at 37 °C. Before the assay, cells were starved for 6 h with EBM-2 medium (Lonza) supplemented with 1% FCS. Stimulation was started by supplementing the EBM-2 medium with 50 ng of the α_2-PI$_{1-8}$-VEGF$_{164}$ liberated from the gels or 50 ng of recombinant mouse VEGF$_{164}$ (Peprotech) as a positive control. Cell numbers were determined 72 h later by adding 10 μl of cell proliferation reagent (WST-1; Roche) to each well. After 4 h of incubation, absorbance of the samples was measured at 650 nm using a microplate reader (Biotek).

Plasma-Leakage Measurements. Evans Blue assays were performed as described previously (5). Four weeks after gel implantation, Evans Blue dye (30 mg/kg of mouse body weight in 100 μL of PBS) (Sigma) was injected into the femoral vein. After 4 h, mice were perfused with 1% paraformaldehyde in 0.05 M citric acid (pH 3.5), and the gastrocnemius muscles were harvested and weighed. Evans Blue was extracted from tissue with formamide at 55 °C overnight and measured with a spectrophotometer at 610 nm. Plasma leakage was expressed as nanograms of extravasated dye per milligram of tissue wet weight ($n = 4$ per group).

Hind-Limb Ischemia Model and Analysis. Experiments were performed at the Ludwig Boltzmann Institute (Vienna), after approval by the local ethical committee. The hind-limb ischemia was performed on female CD1 mice ($n = 11$ per group), weighing 28–36 g (Charles River). Mice were anesthetized with isoflurane (2.5 vol %), and femoral artery ligation and excision were performed unilaterally according to a randomization protocol. Under a surgical microscope, the femoral artery was ligated proximally (inguinal ligament) and distally (bifurcation into saphenous and popliteal artery) and excised. The wound was closed using nonabsorbable sutures in a single-knot technique. The contralateral normally perfused hind limb of each animal served as an internal control. Gels containing either 0 μg/mL, 0.5 μg/mL, or 5 μg/mL α_2-PI$_{1-8}$-VEGF$_{164}$ were injected into the distal part of the quadriceps (50 μL), adductor (30 μL), and biceps femoris (30 μL) thigh muscles of mice according to a randomization protocol. As analgesic treatment, animals received 0.1 mg/kg buprenorphin preoperatively and 1.5 mg/kg meloxicam for the first 3 d after surgery. Hind-limb blood flow was measured by a laser Doppler imaging system (LDI) (Moor Instruments), preoperatively as baseline, postoperatively to assess effective induction of ischemia, and on days 7 and 28. Data analysis was performed with the Moor LDI image processing software (Version 5.3; Moor Instruments). The scan mode was set at 10 ms per pixel, and a resolution of 256 × 256

pixels was chosen. Blood flow was calculated as a ratio of that in the ischemic to that in the contralateral normally perfused hind limbs to account for variables, including ambient light and temperatures, as previously described (7). On day 28, mice were anesthetized with ketamine (67 mg/kg) and xylazine (13 mg/kg) i.p before intravascular systemic perfusion with 1% PFA in PBS (pH 7.4) for 3 min under 120 mm/Hg of pressure. The adductor, biceps, and quadriceps femoris muscles were harvested, postfixed in 0.5% PFA in PBS (pH 7.4) for 2 h at room temperature, cryoprotected in 30% (wt/vol) sucrose in PBS at 4 °C overnight, embedded in OCT compound (CellPath), frozen in freezing isopentane, and cryosectioned.

Tissue sections were analyzed to assess the intramuscular localization of the implanted gel, vessel morphology, and length density as described in *Histological Analyses* and *Vessel Measurements*. After serial sectioning of the entire adductor muscles, the number of collateral arteries was quantified on a single section from each sample, so as to avoid double counting, taken from the proximal part of the muscle in an area remote from the area of injection of the gel and where no angiogenesis was detectable. Collateral vessels >20 μm in diameter were quantified by costaining for CD31 and α-SMA as previously described (8) on three to six random fields per muscle, acquired with a 20× objective on an Olympus BX61 fluorescence microscope (Olympus). Results were expressed as collaterals per field of view ($n = 3$ muscles per group).

Ischemic Wound-Healing Model and Analysis. Experiments were performed at the Ludwig Boltzmann Institute (Vienna), after approval by the local ethical committee. An ischemic wound-healing model was performed on male Sprague–Dawley rats ($n =$ 6 per group), weighing 300–350 g (Harlan-Winkelmann), based on a modified epigastric flap model as previously described (9). Briefly, the rats were anesthetized with ketamine (110 mg/kg) and xylazine (12 mg/kg) i.p. A square skin flap of 8 cm by 8 cm was elevated from cranial to caudal and remained connected to blood circulation only at the caudal base. Half of the flap was rendered ischemic by ligating the left or right inferior neurovascular bundle, and the flap was sutured back. The flap was divided into three vertical zones of equal size, the outer zone on the ligation side reflecting ischemic tissue and the opposite one reflecting vital areas. A 1.5-cm-diameter circular wound was created within the elevated flap in the middle of each outer zone, thus resulting in an ischemic wound on one side and an internal control wound on the opposite side. A volume of 100 μL of optimized-composition gel with 56 μg/mL aprotinin-α_2-PI_{1-8}, either empty or containing 2 μg/mL α_2-PI_{1-8}-$VEGF_{164}$, was applied at the wound sites according to a randomization protocol, allowing solidification in situ. Wounds were covered with a transparent foil dressing (Opsite; Smith and Nephew) and fixed with a second dressing (Fixomull-stretch), changing them on day 1 and 3. As an analgesic treatment, rats received 1.25 mg/kg butorphanol and 0.15 mg/kg meloxicam s.c. on the day of surgery and 3 d later.

Superficial tissue perfusion was measured by a laser Doppler imaging system (Moor Instruments), preoperatively as baseline, postoperatively to assess effective induction of ischemia, and on days 3 and 7. Preoperative baseline values were set at 100%, and subsequent scans were normalized to these values and expressed as a percentage of baseline. The ischemic and nonischemic vertical zones were scanned and evaluated separately. The scan mode was set at 10 ms per pixel, and a resolution of 256 × 256 pixels was chosen. Analyses were made by a software evaluation tool provided with the LDI Moor system (Moor Instruments). Perfusion values were recorded as colored pixels, giving the color-coordinated 2D image of the flap perfusion.

Wound closure was evaluated by planimetric analysis. Excision wounds were traced on a transparent acrylic sheet postsurgery and at days 3 and 7. The sheets were photographed with adjacent standard ruler and analyzed by a planimetric software (Lucia G1, Version 4.8; Laboratory Imaging). The results were expressed as a percentage of the total postoperative wound surface area. On day 7, the animals were euthanized by an intracardiac injection of 150 mg/kg Pentobarbital, and the entire wound areas were excised. Tissues were fixed in 4% (wt/vol) neutral-buffered formalin for 24 h, dehydrated in ascending concentrations of alcohol, embedded in paraffin, and 4-μm-thick sections were cut on a rotary microtome. The samples were warmed to 60 °C for 30 min, deparaffinized in xylene, and rehydrated in graded alcohols. A blocking treatment (1% H_2O_2 in distilled water) to deactivate endogenous peroxidase was performed for 10 min. NG2 staining was performed with 1:100 rabbit anti-rat NG2 antibody (Millipore, Merck) overnight at 4 °C, without epitope retrieval. Samples were rinsed with Tris-buffered saline (TBS) for 5 min and incubated with anti-rabbit antibody labeled with biotin (Dako) for 1 h at room temperature, followed by staining with a biotin substrate kit (VECTASTAIN Elite ABC kit; Vector Labs).

Samples for von Willebrand Factor (vWF) antibody were pretreated with proteinase K (Dako) for 8 min whereas samples for SMA staining underwent heat-induced epitope retrieval for around 20 min at 95 °C in Tris-EDTA buffer (Zytomed). All slides were moved to immunostaining chambers (Coverplate System; Thermo Shandon) and washed with TBS for 5 min. The tissue sections were incubated with 1:100 vWF antibody (polyclonal rabbit anti-human, A0082; Dako) and with 1:5,000 SMA antibody (monoclonal mouse anti-human, A2547; Sigma-Aldrich) for 1 h at room temperature. After rinsing with TBS, anti-mouse or anti-rabbit HRP-labeled micropolymers (Dako) were applied to the slides for 30 min at room temperature, followed by staining with a peroxidase substrate kit (ImmPACT NovaRED; Vector Labs). The slides were then counterstained with hematoxylin, dehydrated, and mounted with Entellan mounting medium (Merck).

Statistics. Data are presented as mean ± SEM. The significance of differences was evaluated using analysis of variance (ANOVA) followed by the Bonferroni test (for multiple comparisons) or using a Mann–Whitney test (for single comparisons), and $P <$ 0.05 was considered statistically significant.

1. Zisch AH, Schenk U, Schense JC, Sakiyama-Elbert SE, Hubbell JA (2001) Covalently conjugated VEGF—fibrin matrices for endothelialization. *J Control Release* 72(1-3): 101–113.
2. Lorentz KM, Kontos S, Frey P, Hubbell JA (2011) Engineered aprotinin for improved stability of fibrin biomaterials. *Biomaterials* 32(2):430–438.
3. Ehrbar M, et al. (2004) Cell-demanded liberation of VEGF121 from fibrin implants induces local and controlled blood vessel growth. *Circ Res* 94(8):1124–1132.
4. von Degenfeld G, et al. (2006) Microenvironmental VEGF distribution is critical for stable and functional vessel growth in ischemia. *FASEB J* 20(14):2657–2659.
5. Ozawa CR, et al. (2004) Microenvironmental VEGF concentration, not total dose, determines a threshold between normal and aberrant angiogenesis. *J Clin Invest* 113(4): 516–527.
6. Largo RA, et al. (2014) Long-term biostability and bioactivity of "fibrin linked" VEGF121 in vitro and in vivo. *Biomater. Sci.* 2(4):581–590.
7. Couffinhal T, et al. (1998) Mouse model of angiogenesis. *Am J Pathol* 152(6): 1667–1679.
8. Heeschen C, et al. (2001) Nicotine stimulates angiogenesis and promotes tumor growth and atherosclerosis. *Nat Med* 7(7):833–839.
9. Michlits W, Mittermayr R, Schäfer R, Redl H, Aharinejad S (2007) Fibrin-embedded administration of VEGF plasmid enhances skin flap survival. *Wound Repair Regen* 15 (3):360–367.

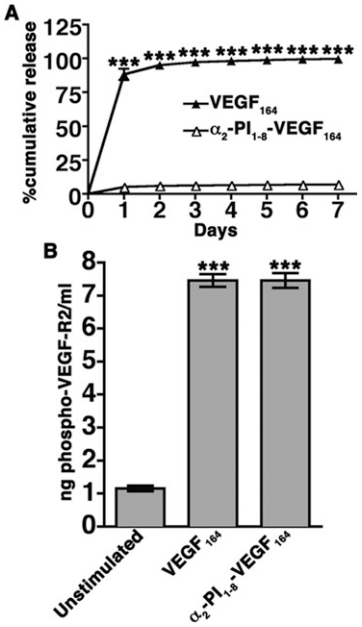

Fig. S1. Characterization of the fusion protein α_2-$PI_{1–8}$-$VEGF_{164}$. (*A*) Percent cumulative release of α_2-$PI_{1–8}$-$VEGF_{164}$ and native $VEGF_{164}$ from fibrin gels. The quantity of native and variant $VEGF_{164}$ was measured on buffer collected and replaced daily for 7 d by ELISA. Values are reported as mean ± SEM ($n = 3$). (*B*) Phosphorylation assay. Serum-starved HUVECs were incubated with 50 ng/mL native $VEGF_{164}$ or α2-PI_{1-8}-$VEGF_{164}$, and the amount of phosphorylated VEGF-Receptor 2 (VEGF-R2) was quantified by ELISA (ng/mL). Values are reported as mean ± SEM ($n = 3$); ***$P < 0.001$.

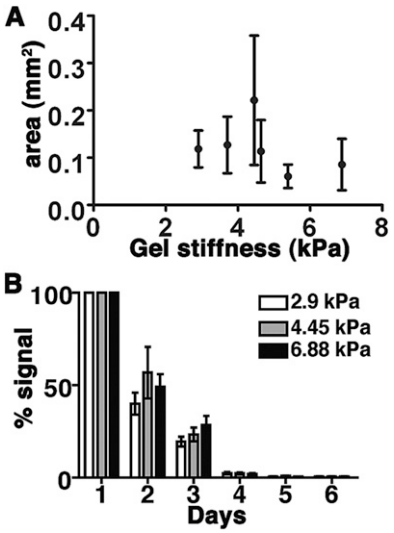

Fig. S2. In vivo gel degradation. (*A*) Gel compositions of different stiffness were injected into the gastrocnemius muscles of SCID mice. Immunofluorescence staining of serial tissue sections with a fibrin-specific antibody showed no significant differences in the amount of remaining gel 4 d after injection. Results are shown as mean gel area (mm^2) ± SEM ($n = 3$). (*B*) Different gel compositions spanning the whole range of stiffnesses were prepared with fluorescently labeled fibrinogen and injected into gastrocnemius muscles. The degradation was monitored in vivo daily for a period of 9 d by noninvasive imaging of fibrin fluorescence. Results are shown as percentage of the initial fluorescent signal remaining over time (mean ± SEM; $n = 9$).

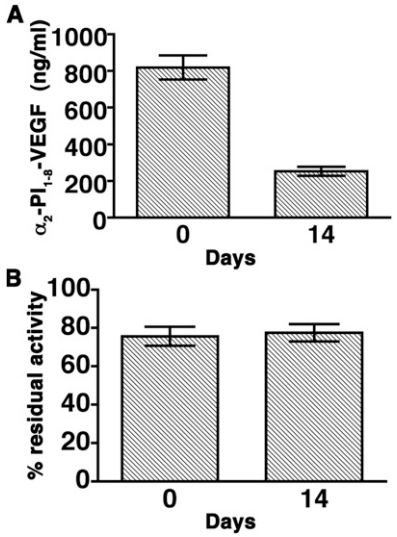

Fig. S3. The biological activity of α_2-PI$_{1-8}$-VEGF$_{164}$ is preserved after 2 wk of in vivo implantation. Fibrin gels of 20 μL volume containing 100 μg/mL α_2-PI$_{1-8}$-VEGF$_{164}$ and 56 μg/mL aprotinin-α_2-PI$_{1-8}$ were preformed in vitro and frozen at −80 °C either immediately (day 0) or 2 wk after s.c. implantation into nude mice (day 14). (*A*) After digestion with plasmin for ∼56 h at 37 °C, the amount of extracted α_2-PI$_{1-8}$-VEGF$_{164}$ was measured by ELISA. Results are shown as mean concentration in the extraction supernatant (ng/mL) ± SEM (n = 4). (*B*) The biological activity of the extracted α_2-PI$_{1-8}$-VEGF$_{164}$ was determined in a HUVEC proliferation assay. Recombinant fresh VEGF$_{164}$ was used as positive control. Results are shown as the percentage residual activity in cell proliferation compared with fresh recombinant VEGF, set at 100% (mean ± SEM; n = 4).

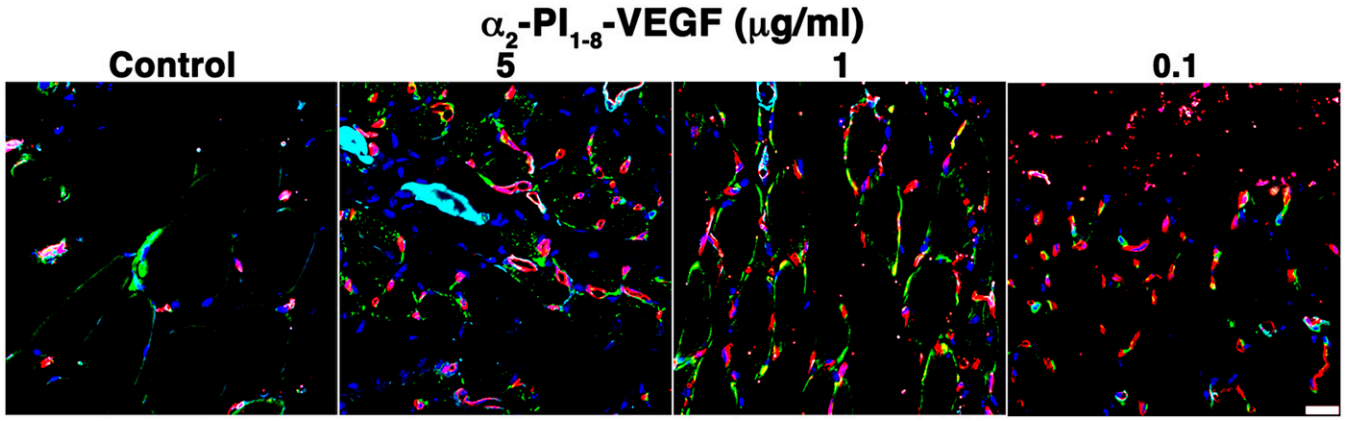

Fig. S4. A wide range of α_2-PI$_{1-8}$-VEGF$_{164}$ doses induces robust and normal angiogenesis. Fibrin gels containing 56 μg/mL aprotinin-α_2-PI$_{1-8}$ and 0 μg/mL (negative control), 5 μg/mL, 1 μg/mL, or 0.1 μg/mL α_2-PI$_{1-8}$-VEGF$_{164}$ were injected into the gastrocnemius muscles of SCID mice. Tissues were analyzed 9 d later, and frozen sections were immunostained to detect endothelial cells (CD31, in red), pericytes (NG2, in green), smooth-muscle cells (α-SMA, in cyan), and nuclei (DAPI, in blue). n = 3. (Scale bar: 20 μm.)

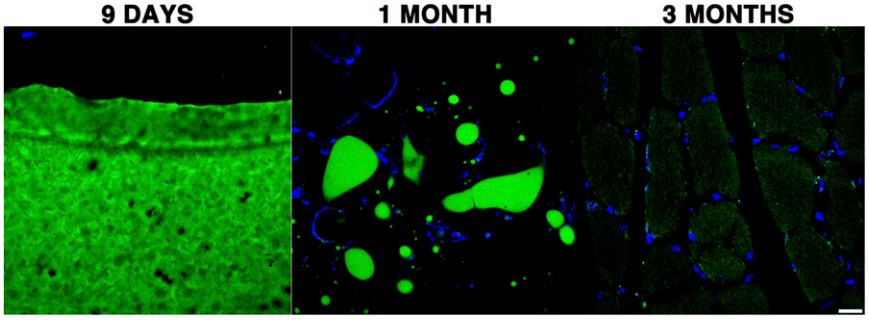

Fig. S5. In vivo persistence of optimized fibrin gels. Fibrin gels containing 56 μg/mL aprotinin-α_2-PI$_{1-8}$ and 0.1 μg/mL α_2-PI$_{1-8}$-VEGF$_{164}$ were injected into the gastrocnemius muscles of SCID mice. Tissues were analyzed 9 d, 1 mo, or 3 mo later, and frozen sections were immunostained to detect fibrin (anti-fibrin antibody, in green) and nuclei (DAPI, in blue). Abundant gel is visible 9 d after injection whereas, after 4 wk, small residues are still present and none is detectable after 3 mo. (Scale bar: 20 μm.)

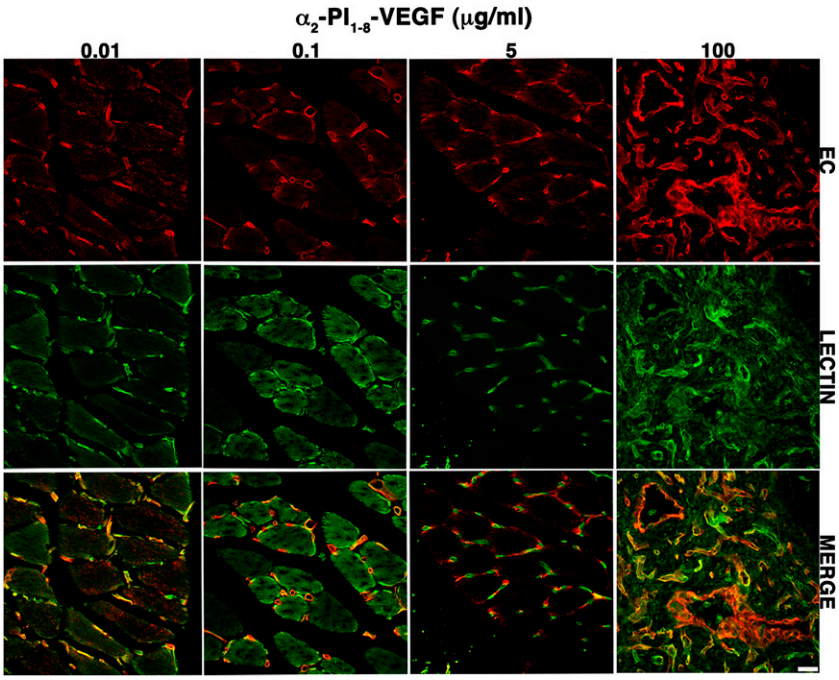

Fig. S6. Vessels induced by α_2-$PI_{1–8}$-$VEGF_{164}$ are functionally perfused after 4 wk. Fibrin gels containing 56 μg/mL aprotinin-α_2-$PI_{1–8}$ and 0.01 μg/mL, 0.1 μg/mL, 5 μg/mL, and 100 μg/mL α_2-$PI_{1–8}$-$VEGF_{164}$ were injected into gastrocnemius muscles of SCID mice. FITC-lectin was injected i.v. into mice 4 wk later, just before euthanizing. Endothelial structures (EC) were stained with an antibody against CD31 (red) whereas FITC-lectin is shown in green. Perfused vessels were identified as staining positive for both CD31 and FITC-lectin. $n = 3$. (Scale bar: 20 μm.)

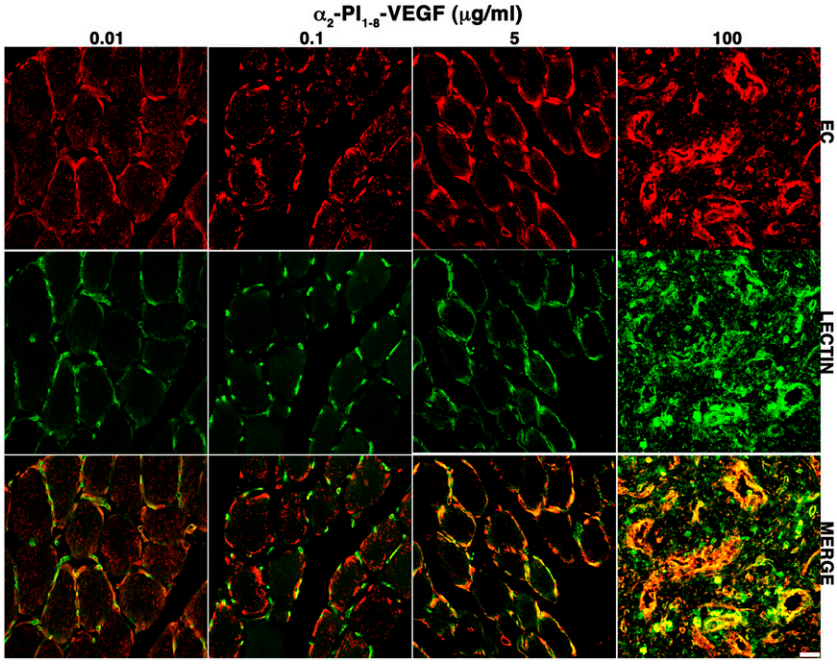

Fig. S7. Vessels induced by α_2-$PI_{1–8}$-$VEGF_{164}$ are functionally perfused after 3 mo. Fibrin gels containing 56 μg/mL aprotinin-α_2-$PI_{1–8}$ and 0.01 μg/mL, 0.1 μg/mL, 5 μg/mL, and 100 μg/mL α_2-$PI_{1–8}$-$VEGF_{164}$ were injected into gastrocnemius muscles of SCID mice. FITC-lectin was injected i.v. into mice 3 mo later, just before euthanizing. Endothelial structures (EC) were stained with an antibody against CD31 (red) whereas FITC-lectin is shown in green. Perfused vessels were identified as staining positive for both CD31 and FITC-lectin. $n = 3$. (Scale bar: 20 μm.)

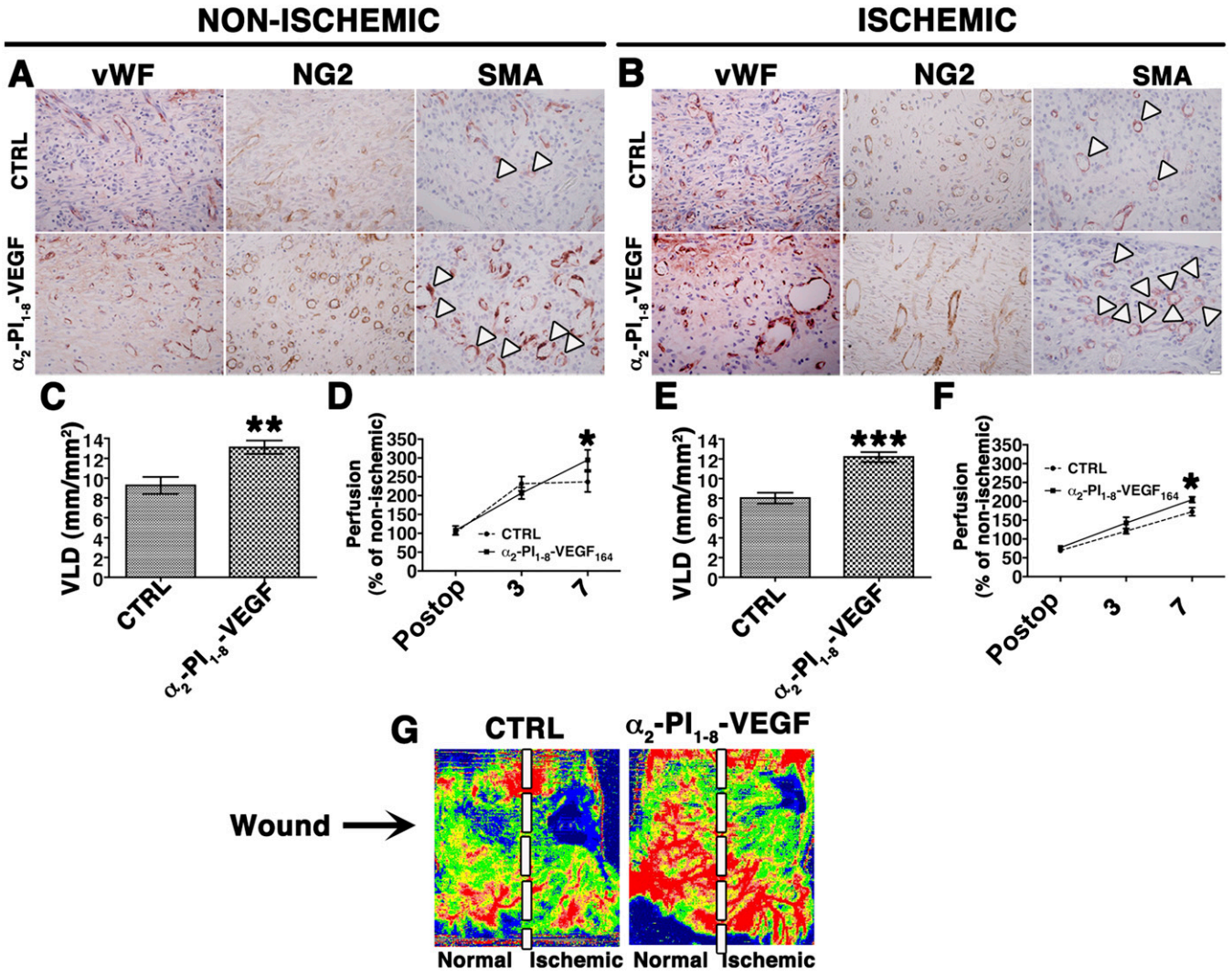

Fig. S8. α_2-PI$_{1-8}$-VEGF$_{164}$ significantly improves angiogenesis and tissue perfusion in an ischemic wound-healing model. Fibrin gels containing 56 μg/mL aprotinin-α_2-PI$_{1-8}$ alone (CTRL) or with 2 μg/mL α_2-PI$_{1-8}$-VEGF$_{164}$ were placed on circular wounds in either nonischemic or ischemic dorsal skin flaps in Sprague–Dawley rats. (*A* and *B*) Tissues were harvested 7 d later, and paraffin sections were immunostained to detect endothelial cells [von Willebrand Factor (vWF)], pericytes (NG2), and smooth-muscle cells (SMA). $n = 6$. (Scale bar: 20 μm.) Arrowheads, α-SMA–positive microvessels and small-caliber arterioles and venules. (*C* and *E*) The amount of angiogenesis was quantified as vessel length density (VLD), and results are shown as mean ± SEM ($n = 5$–10 fields per group); ***$P < 0.001$, **$P < 0.002$. (*D* and *F*) Tissue blood perfusion was quantified by laser Doppler imaging after flap elevation with (*F*) or without (*D*) arterial ligation [postoperative (postop)] and 3 d and 7 d after gel implantation. Results show the amount of perfusion as a percentage of the nonischemic baseline set at 100% (mean ± SEM; $n = 6$); *$P < 0.05$. (*G*) Representative laser Doppler images of nonischemic and ischemic wounds (*Left* and *Right* side of each image, respectively) 7 d after treatment with control gels (CTRL) or α_2-PI$_{1-8}$-VEGF$_{164}$.

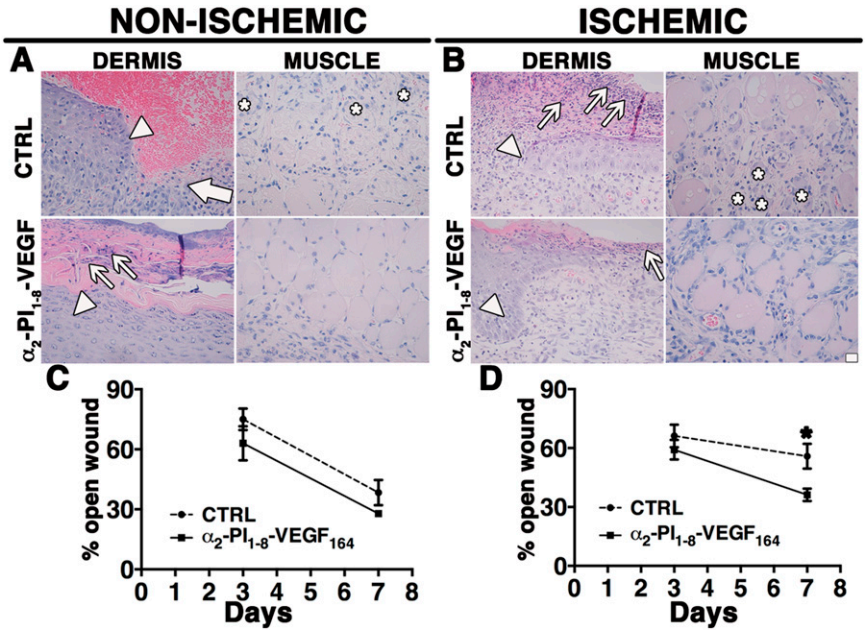

Fig. S9. α_2-PI_{1-8}-$VEGF_{164}$ significantly improves wound regeneration in an ischemic wound-healing model. Fibrin gels containing 56 μg/mL aprotinin-α_2-PI_{1-8} alone (CTRL) or with 2 μg/mL α_2-PI_{1-8}-$VEGF_{164}$ were placed on circular wounds in either nonischemic or ischemic dorsal skin flaps in Sprague–Dawley rats. (*A* and *B*) Tissues were harvested 7 d later, and paraffin sections were stained with H&E. Images were acquired both in the superficial layer (DERMIS) and in the underlying muscle layer (MUSCLE). $n = 6$. (Scale bar: 20 μm.) Arrowheads, epidermal hyperplasia; thick arrow, bleeding area; asterisks, monocyte infiltration of muscle fibers; thin arrows, keratinized tissue with apoptotic bodies. (*C* and *D*) Wound healing was measured by planimetric analysis 3 and 7 d after gel implantation, and results show the size of still-open wounds as a percentage of the initial size at day 0, set at 100% (mean ± SEM; $n = 6$); $^*P < 0.05$.